THE JOURNAL OF BIOLOGICAL CHEMISTRY VOL. 290, NO. 7, pp. 4356–4366, February 13, 2015

An Alternative Retinoic Acid-responsive *Stra6* Promoter Regulated in Response to Retinol Deficiency*

Received for publication, September 23, 2014, and in revised form, December 25, 2014 Published, JBC Papers in Press, December 28, 2014, DOI 10.1074/jbc.M114.613968

Kristian B. Laursen[‡], **Vasundhra Kashyap**[‡], **Joseph Scandura**[§], **and Lorraine J. Gudas**[‡§1]

From the [‡]*Pharmacology Department and the* [§]*Department of Medicine, Weill Cornell Medical College of Cornell University, New York, New York 10065*

Background: Stra6 is a trans-membrane retinol transporter involved in retinoic acid (RA) signaling.
Results: The epigenetic signature of the *Stra6* gene reveals an RA-responsive element.
Conclusion: An intragenic RARE drives RA-responsive expression of two different *Stra6* isoforms.
Significance: The novel, shorter *Stra6* transcript may encode a functionally different retinol transporter.

Cellular uptake of vitamin A (retinol) is essential for many biological functions. The Stra6 protein binds the serum retinol-binding protein, RBP4, and acts in conjunction with the enzyme lecithin:retinol acyltransferase to facilitate retinol uptake in some cell types. We show that in embryonic stem (ES) cells and in some tissues, the *Stra6* gene encodes two distinct mRNAs transcribed from two different promoters. Whereas both are all-*trans*-retinoic acid (RA)-responsive in ES cells, the downstream promoter contains a half-site RA response element (RARE) and drives an ~13-fold, RA-associated increase in luciferase reporter activity. We employed CRISPR-Cas9 genome editing to show that the endogenous RARE is required for RA-induced transcription of both *Stra6* isoforms. We further demonstrate that in ES cells, 1) both RARγ and RXRα are present at the *Stra6* RARE; 2) RA increases co-activator p300 (KAT3B) binding and histone H3 Lys-27 acetylation at both promoters; 3) RA decreases Suz12 levels and histone H3 Lys-27 trimethylation epigenetic marks at both promoters; and 4) these epigenetic changes are diminished in the absence of RARγ. In the brains of WT mice, both the longer and the shorter *Stra6* transcript (*Stra6*$_L$ and *Stra6*$_S$, respectively) are highly expressed, whereas these transcripts are found only at low levels in RAR$\gamma^{-/-}$ mice. In the brains of vitamin A-deficient mice, both *Stra6*$_L$ and *Stra6*$_S$ levels are decreased. In contrast, in the vitamin A-deficient kidneys, the *Stra6*$_L$ levels are greatly increased, whereas *Stra6*$_S$ levels are decreased. Our data show that kidneys respond to retinol deficiency by differential *Stra6* promoter usage, which may play a role in the retention of retinol when vitamin A is low.

The plasma retinol-binding protein (RBP4)[2] binds to a thyroxine transthyretin (TTR)-binding protein in a 1:1 stoichiometry to deliver and distribute vitamin A (all-*trans*-retinol) to many cell types in the body (for a review, see Ref. 1). An RBP4 receptor protein, stimulated by retinoic acid 6 (Stra6), binds RBP4 and allows uptake of the liganded, holo-RBP complex into some cell types (2, 3). A second RBP4 receptor (RBPR2) with structural similarities to Stra6 was recently identified in liver (4). In addition to Stra6, the enzyme lecithin:retinol acyltransferase (LRAT) was reported to play a key role in the uptake of retinol into certain cell types (2, 5–11). Uptake of retinol from RBP4 requires a functional interaction between LRAT and Stra6 (10).

Stra6 transcripts and protein are expressed in many tissues involved in retinol actions, such as the placenta, testis, skin, kidney, eye, brain, and choroid plexus (12, 13). *Stra6* is involved in cell proliferation control, and knockdown of *Stra6* in skin epithelia leads to aberrant hyperproliferation (14). The Stra6 protein can function as a cytokine receptor that activates Jak/Stat signaling in response to retinol-RBP4 complexes. Thus, retinol and RBP4 can influence transcription via Stra6 and subsequent activation of the transcription factor Stat5 (15, 16). Additionally, Stra6, when bound to the retinol-RBP4 complex, allows recruitment of an intracellular binding protein for retinol, the cellular retinol binding protein 1 (CRBP-1) (17). Stra6 also functions to regulate other biological activities, such as adipogenesis (19), lipid metabolism (15), and p53-induced apoptosis after DNA damage (18). Because TTR prevents Stra6 from associating with the RBP4-retinol complex, Stra6 is activated by retinol only when the plasma RBP4 level is higher than the level of TTR (17). This finding implicates TTR in the regu-

* This work was supported, in whole or in part, by National Institutes of Health, NCI, Grant R01 CA043796 (to L. J. G.). This work was also supported by Weill Cornell funds.

[1] To whom correspondence should be addressed: Dept. of Pharmacology, Weill Cornell Medical College, New York, New York 10065. Tel.: 212-746-6250; Fax: 212-746-8858; E-mail: ljgudas@med.cornell.edu.

[2] The abbreviations used are: RBP4, serum retinol-binding protein (NCBI gene ID: 19662); 36B4, ribosomal protein large P0 (NCBI gene ID: 11837); H3K27, histone H3 Lys-27; H3K27ac, H3K27 acetylation; H3K27me3, H3K27 trimethylation; H3K4me3, histone H3 Lys-4 trimethylation; H3K9/14ac, histone H3Lys-9/14 acetylation; CRBP-1, cellular retinol-binding protein 1 (NCBI gene ID: 19659); ES, embryonic stem; HPRT1, hypoxanthine guanine phosphoribosyl transferase 1 (NCBI gene ID: 15452); LRAT, lecithin:retinol acyltransferase (NCBI gene ID: 79235); p300, KAT3B (NCBI gene ID: 328572); P_L, $Promoter_{Long}$; P_S, $Promoter_{Short}$; RA, retinoic acid; RAR, retinoic acid receptor; RARE, retinoic acid response element; RARα, retinoid acid receptor α (NCBI gene ID: 19401); RARβ, retinoid acid receptor β (NCBI gene ID: 218772); RARγ, retinoid acid receptor γ (NCBI gene ID: 5916); RBPR2, serum retinol-binding protein receptor 2 (NCBI gene ID: 74152); RXRα, retinoid X receptor α (NCBI gene ID: 20181); RefSeq, NCBI reference sequence; Ring1B, ring finger protein 1B (NCBI gene ID: 19821); Stra6, stimulated by retinoic acid 6 (NCBI gene ID: 20897); Suz12, suppressor of zeste 12 homolog (NCBI gene ID: 52615); TSS, transcriptional start site; TTR, thyroxine transthyretin (NCBI Gene ID: 22139); VAD, vitamin A (retinol)-deficient diet; VAS, vitamin A (retinol)-sufficient diet; MLL, mixed-lineage leukemia; PolII, RNA polymerase II.

lation of Stra6 signaling. In adipocyte precursor cells, Stra6 mediates bidirectional retinol transport, depending on whether RBP4 is retinol-bound (19).

Mutations in *STRA6* can result in the Matthew-Wood syndrome, which consists of severe microphthalmia, pulmonary agenesis, bilateral diaphragmatic eventration, duodenal stenosis, pancreatic malformations, and growth retardation (13, 20, 21). Some mutations in *STRA6* in humans involve either a homozygous insertion/deletion in exon 2 or a homozygous insertion in exon 7, predicting a premature stop codon (20). Several *STRA6* mutations associated with human disease have been shown to limit or abolish retinol uptake into cells (23, 24). Three groups have independently reported marked ocular defects in *Stra6* null mice (25–27). Genetic ablation of *Stra6* results in a reduced retinoid content in the retinal pigment epithelium and neurosensory retina (greater than a 95% reduction in retinyl esters) with consequently fewer cone photoreceptor cells and diminished cone b-wave amplitude (25). Under the evaluated conditions, knock-out of *Stra6* did not impair the physiological functions of retinoids in tissues other than the eye (26). Under vitamin A-deficient conditions, Stra6 was reported to facilitate redistribution from storage tissue (*e.g.* liver and lungs) to the eye (27), possibly in conjunction with the recently identified RBPR2, another RBP4 receptor (4). Ablation of *Stra6* can also protect animals from the insulin-resistant state induced by feeding a high fat, high sucrose diet (28), which may be a result of impaired Jak/Stat signaling (29). Why humans with certain mutations in *STRA6* exhibit a more severe morphological phenotype (25–27) than the *Stra6* knock-out mice is currently not understood.

Vitamin A acts through its biologically active metabolite, all-*trans*-retinoic acid (RA), and the retinoic acid receptors (RARs) to regulate large numbers of genes at the transcriptional level in various cell types (30–32). On a molecular level, RA mediates major changes in epigenetic marks on specific target genes (33–37). We recently showed that *Stra6* transcripts are increased by RA treatment of embryonic stem (ES) cells and that this induction depends on RARγ (38).

There is a great interest in the cellular uptake of vitamin A, yet the mechanisms by which the *Stra6* gene is regulated at the transcriptional level are not clearly defined. In this report, we demonstrate that the *Stra6* gene possesses two different promoters, both of which are induced by RA through a single intragenic RARE. We characterize the *Stra6* retinoic acid-responsive DNA element (RARE) and demonstrate that RXRα/RARγ heterodimers directly associate with this cis-acting element of *Stra6* to activate RA-dependent transcription. Finally, we identify the differential regulation of the two *Stra6* promoters in the kidneys of vitamin A-deficient animals, which points to physiologically distinct functions of the two *Stra6* isoforms.

EXPERIMENTAL PROCEDURES

Cell Culture and Retinoic Acid Treatment of ES Cells—The WT (CCE) and RAR$\gamma^{-/-}$ ES cell lines were derived and cultured as described (33). RA (Sigma) was added to the cells 24 h after plating (1 μM final concentration), and ethanol (EtOH, 0.1%) served as a vehicle control. For time course evaluations, ES cells were plated in gelatin-coated tissue culture dishes and treated with RA (1 μM) at various time points up to 72 h prior to harvesting.

Vitamin A-deficient Mice—WT C57Bl/6 and LRAT null C57Bl/6 mice were given vitamin A-sufficient (VAS) or vitamin A-deficient (VAD) chow for 10 weeks, as described (6). The treatment of the mice was approved by the Institutional Animal Care and Use Committee at Weill Cornell. Tissues were harvested, RNA was isolated, and semiquantitative RT-PCR was performed as described (6). The brains were dissected without the eyes. Serum and liver retinoid levels were measured by HPLC as described (6), demonstrating that the mice on the VAD chow were vitamin A-deficient.

RNA Isolation and Reverse Transcription—Total RNA was isolated from F9 and ES cells using TRIzol reagent (Invitrogen), and RNA was quantitated by optical density at 260 nm. The RNA (1 μg) was reverse transcribed (Quanta Biosciences, Gaithersburg, MD) and then diluted 1:10 with H_2O. The cDNA obtained was diluted 10-fold, and 3 μl of this cDNA was utilized for PCRs.

Generation of cDNA, Semiquantitative, and Real-time PCR—Real-time PCR was performed using SYBR Green Supermix (Quanta Biosciences) in a 15-μl reaction containing reaction mix (1×), a 0.2 μM concentration of each primer, and 3 μl of cDNA template. The reactions were run on a Bio-Rad MyiQ^{TM} single color real-time PCR detection system (Bio-Rad). Amplification in the linear range was demonstrated by a serial dilution of cDNA from RA-treated wild type (WT) cells included in each reaction (1:1, 1:5, 1:10, 1:50, 1:100, and 1:500). Reactions with H_2O and template without reverse transcriptase, respectively, served as negative controls for primer-dimer and for amplification of residual genomic DNA. All real-time PCR primers were designed to span intronic regions. Primer sequences are listed (Table 1). Each expression analysis was performed at least three times (e.g. n≥3, independently propagated cells, experiment repeated three times). Within each PCR analysis, samples were run in triplicate. PCR products were verified by DNA sequencing.

Mapping of Transcriptional Start Sites—5′-Rapid amplification of cDNA ends (RACE) was performed with the Roche Applied Science 5′/3′ RACE kit using mStra6(−)J for cDNA synthesis and mStra6(−)B for nested PCR amplification. The PCR products were purified using a PCR purification kit (Qiagen), and the eluted DNA was recovered by ligation into the pGEM-T easy vector (Promega, WI). The ligated products were recovered by bacterial transformation. Single colonies were picked, and plasmid DNA was isolated. Insert-containing plasmids were identified by restriction digestion and sequenced using T7(+) and SP6(+) primers.

Constructing and Assaying Stra6 Reporter Plasmids—Firefly luciferase reporter constructs were designed by cloning PCR fragments of various Stra6 genomic regions into the pGL3 reporter plasmid. In brief, PCR fragments were SpeI/SalI-digested and cloned into NheI/XhoI sites of the pGL3 basic plasmid (Promega, WI). The *Stra6* reporter constructs and their genomic coordinates are shown in Table 2. Point mutations were introduced into the pGL3 mStra6–0.8 construct using Stratagene QuikChange (see Table 1 for primer sequences). The ES cells were transiently transfected with different luciferase reporter constructs using Lipofectamine LTX (Invitrogen). The pRL-TK reporter plasmid,

TABLE 1
Primer sequences

Forward	Sense primer (5'-3')	Reverse	Antisense primer (5'-3')	Product cDNA	(bp) gDNA
mStra6(+)A	CCTCCGGGGTGACAGATGACTAC	mStra6(-)B	AGCTTCCAGGGCCCTCTTGATGT	406	n/a
mStra6(+)I	CTGACTGACTGCCTTCCTTCT	mStra6(-)B	AGCTTCCAGGGCCCTCTTGATGT	220	n/a
mStra6(+)A	CCTCCGGGGTGACAGATGACTAC	mStra6(-)D	CAGGAATCCAAGACCCAGAA	620	7848
mStra6(+)O	ACCACTGCCTTTCCTGAACCT	mStra6(-)D	CAGGAATCCAAGACCCAGAA	290	2462
mStra6(+)P	CAGTTTAGGGAGCACACTGTATA	mStra6(-)D	CAGGAATCCAAGACCCAGAA	475	2645
mStra6(+)C	GTTCAGGTCTGGCAGAAAGC	mStra6(-)D	CAGGAATCCAAGACCCAGAA	102	1794
Controls					
m36B4(+)A	AGAACAACCCAGCTCTGGAGAAA	m36B4(-)B	ACACCCTCCAGAAAGCGAGAGT	448	629
mHPRT1(+)A	GCTTGCTGGTGAAAAGGACCTCTCGAAG	mHPRT1(-)B	CCCTGAAGTACTCATTATAGTCAAGGGCAT	117	288
mLRAT(+)C	CTGACCAATGACAAGGAACGCACTC	mLRAT(-)B	ATGGGATACAGATTGCAGGAAGGG	430	6474
mRARαE34(+)	TGGCTCAAACCACTCCATCGAGA	mRARαE6(-)	CCTGGTGCGCTTTGCGAACC	425	n/a
mRARβE3(+)	GCAGCACCGGCATACTGCTC	mRARβE4(-)	CACTGACGCCATAGTGGTA	155	n/a
mRARγE45(+)	TGCCAGTCTACAATCGGTGGA	mRARγE6(-)	GATACAGTTTTTGTCACGGTGACAT	229	n/a
ChIP					
mStra6-p(+)A	TGGAGAATACTGAGCATTG	mStra6-p(-)B	TCACCATCCTAGAACACT	n/a	78
mStra6-R(+)G	AAAGCAGCGATAAAGTAG	mStra6-R(-)H	AGTTACCTCTTGATGTCT	n/a	116
Construction					kb
mStra6-R(+)S	tccactagtGATGCAGGAAGAAGTCT	mStra6-R(-)T	tttgtcgacCCAAGAAATCCACAGGGCTGTCA		0.5
		mStra6(-)0.6	tttgtcgacCACAAAGACAGCAGCAGGCACTGT		0.6
		mStra6(-)0.8	tttgtcgacGTTCTCTCTATTGTAAACTAGAGCT		0.8
		mStra6(-)0.9	tttgtcgacTGCTTTCTTCTCTGACCCTTGGTT		0.9
		mStra6-R(-)S	tttgtcgacAGTTACCTCTTGATGTCT		1.0
		mStra6-i(-)S	tttgtcgacGCTGTGAAACTGGATTGTCTGTCTA		1.7
Mut1(+)	ACTGCCTTTCCactACCTCACTGCA	Mut1(-)	TGCAGTGAGGTagtGGAAAGGCAGT		n/a
Mut2(+)	TGGCCGCAGAAactCCTCTTTAGAT	Mut2(-)	ATCTAAAGAGGagtTTCTGCGGCCA		n/a
5'RACE and Genome Editing				short	long
Anchor-dT	GACCACGCGTATCGATGTCGACT$_{14}$VN	mStra6(-)B	AGCTTCCAGGGCCCTCTTGATGT	260	520
Anchor	GATTGACCACGCGTATCGATGT	mStra6(-)J	GCAGAGAAGAGTTCTCAGATACTT	590	850
Cas9S6R(+)	CACCGTGGAGACTGTTGATCTAAAG	Cas9S6R(-)	AAACCTTTAGATCAACAGTCTCCAC		

TABLE 2
***Stra6* reporter constructs and luciferase data**
Increase in luciferase activity upon 24-h RA treatment (relative to vehicle-treated cells). Shown are genomic coordinates for *Stra6* reporter elements and the RARE (mm9). Note that pGL3 Stra6-P_L/P_S is a composite reporter construct that contains two *Stra6* genomic regions (one upstream and one downstream of the luciferase coding region). These constructs are further described in the legend to Fig. 2*A*.

pGL3 construct	RA-responsive (Luc RA/control)	Genomic coordinates			
		Chromosome	Strand	Start	End
	Fold increase				
Stra6-P_L	2.3	9	+	57976612	57977225
Stra6-P_L/P_S	1.4	9	+	57976612	57977225
				57988013	57989474
Stra6-1.7	3.9	9	+	57987743	57989474
Stra6-1.0	5.8	9	+	57987743	57988689
Stra6-0.9	14.9	9	+	57987743	57988585
Stra6-0.8	13.4	9	+	57987743	57988564
Stra6-0.6	2.1	9	+	57987743	57988278
Stra6-0.5	2.2	9	+	57987743	57988237
RARE	Inverted repeat	9	+	57988490	57988511

Renilla luciferase-thymidine kinase (Promega, WI), served as a control for transfection efficiency. WT ES cells were transfected and then cultured in DME containing 1.0 μM RA for 8 or 24 h, as indicated. Firefly and *Renilla* luciferase activities were sequentially measured with a luminometer using the Dual-Luciferase reporter assay system (Promega).

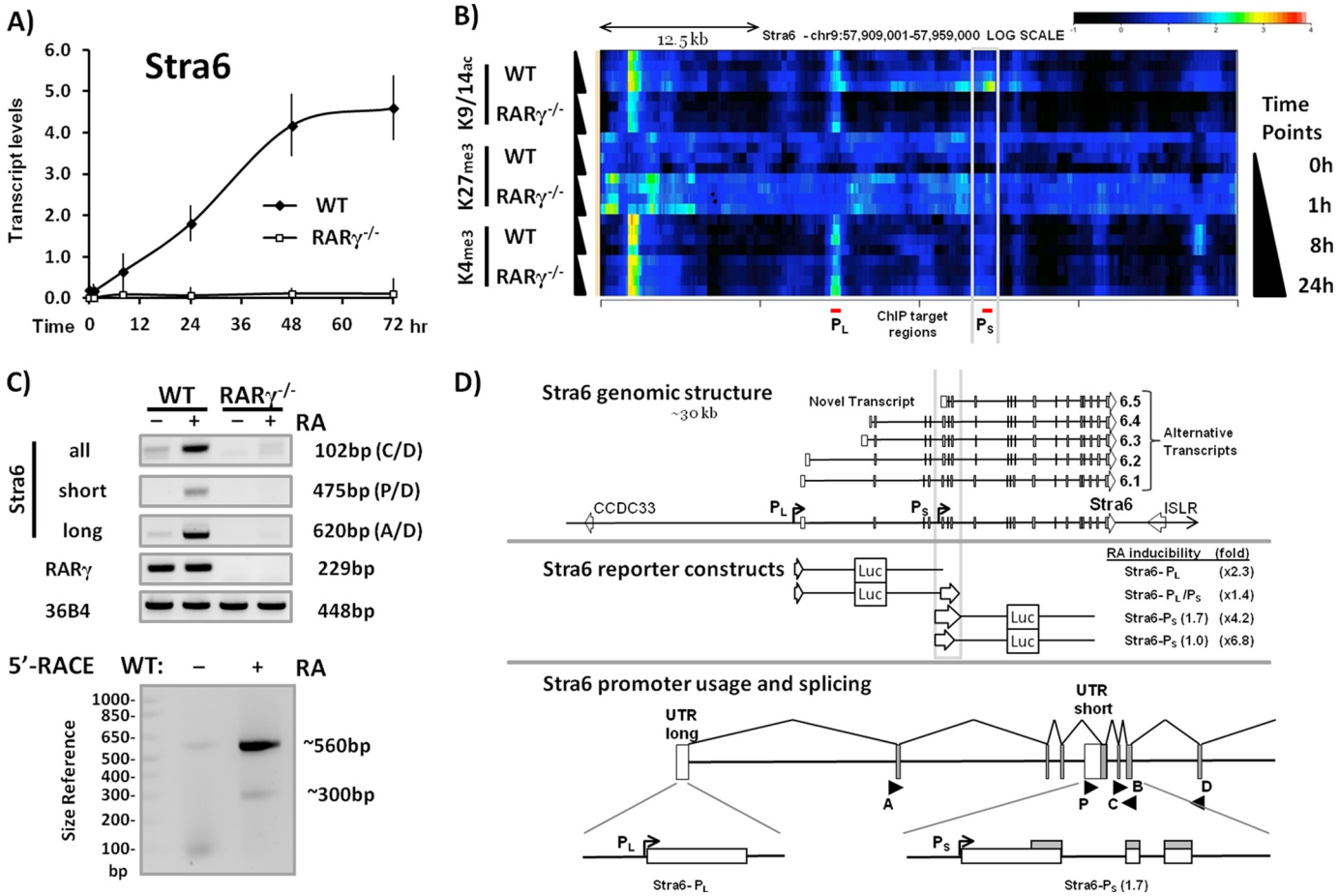

FIGURE 1. **RA-responsiveness of *Stra6* in WT and *RARγ*$^{-/-}$ ES cells.** *A*, in WT but not in *RARγ*$^{-/-}$ ES cells, *Stra6* transcript levels (total) increase with the duration of RA exposure (1 μM). *B*, heat map of *Stra6* epigenetic signatures (H3K9/14ac, H3K27me3, and H3K4me3) in WT and *RARγ*$^{-/-}$ ES cells upon RA exposure for 1, 8, and 24 h (relative to vehicle-treated control). The intensity of the heat map specifies the levels of epigenetic marks (represented by the *scale bar* at the *top right*, *red/white*, *highest*). The promoter regions P_L and P_S correspond to the P_{RefSeq} and to the novel promoter proximal to the *Stra6* RARE, respectively. Note that the heat map is aligned with the schematics in *D below*. *C*, detection of *Stra6* transcripts from P_L and P_S promoters as well as total *Stra6* transcript levels in untreated and RA-treated WT and *RARγ*$^{-/-}$ ES cells by RT-PCR (*top*). The primers utilized are specified by *letters*. *RARγ* transcript levels and 36B4 (loading control) are also shown. *Bottom*, mapping the 5′-end of RA-induced *Stra6* transcripts by 5′-RACE. *D*, *Stra6* genomic structure (*top*), reporter constructs (*middle*), and promoter diagram (*bottom*). Alternative transcripts and *Stra6* genomic regions are depicted at the *top*. The RefSeq promoter (P_L) and the novel RA-responsive promoter (P_S) identified are shown here. *Squares*, exons (*open*, untranslated). *Stra6* reporter constructs were evaluated for RA induction of P_L and P_S (-fold induction by RA is noted to the *right*). The alternative *Stra6* transcripts correspond to NM_001162475.1 (*6.1*), NM_009291.2 (*6.2*), NM_001162476.1 (*6.3*), NM_001162479.1 (*6.4*), and a novel short isoform (*6.5*; GenBank™ number AK092227.1). *Stra6* promoter regions (P_L and P_S) and exon usage of the 5′-mRNAs are shown. The locations of primer binding sites are specified by *single letters below* or *above* the *arrowheads* (forward and reverse primers, respectively). *Error bars*, S.E.

Genome Editing and Screening—Double-stranded DNA fragments targeting the *Stra6*-RARE (Table 1) were cloned into the pX330 vector (39). Integrity of the insert was confirmed by sequencing, and the construct was transfected into WT ES cells. Upon overnight recovery, the transfected cells were reseeded at low density (2×10^3 cells/15-cm dish) to obtain independent clonal lines. The colonies were screened by PCR (mStra6(+)P and mStra6-R(−)H primers) followed by MboI restriction digest. The PCR bands with modified MboI sites were sequenced to map the exact mutations introduced at the *Stra6*-RARE. Cell lines with single and double mutations of the *Stra6*-RARE were assayed in three independent experiments for transcriptional induction of *Stra6* by RA.

Chromatin Immunoprecipitation (ChIP) Assays—A one-step ChIP protocol that utilizes formaldehyde cross-linking was employed for histone ChIP assays. For active RNA polymerase II (PolII) and transcription factor ChIP assays (PolII-CTD, Suz12, and Ring1B), we used a two-step ChIP protocol where the formaldehyde cross-linking is preceded by a disuccinimidyl glutarate cross-linking step (40–42). ChIP assays were performed on 5.0×10^5 sonicated ES cells using 2 μg of antibody/immunoprecipitation. The assays were performed on at least three samples from independent experiments (*e.g.* independently propagated cells). Antibodies used were as follows: H3K27me3 (07-449, Millipore); H3K27ac (07-360, Millipore); PolII-CTD (MMS-134R, Covance, Princeton, NJ); RARγ (ab12012, Abcam, MA); RXRα (D-20, sc-553, Santa Cruz Biotechnology, Inc.); Suz12 (3737S, Millipore, MA); p300 (N-15, sc-584, Santa Cruz Biotechnology); rabbit IgG (sc-2027, Santa Cruz Biotechnology). The ChIP-on-chip assays were performed as described (33).

Data Analysis and Statistics—Data from at least three independent experiments were analyzed using one-way analysis of variance in the expression and ChIP analyses. The S.E. was determined for each of the data sets (at least three biological, indepen-

dent repeats, each in triplicate, plotted as *error bars* in the graphs), and analysis of variance values of $p < 0.05$ among compared samples were assigned statistical significance.

RESULTS

The Increase in Stra6 Transcripts in RA-treated ES Cells Is Associated with Extensive Epigenetic Changes—We employed WT and *RARγ*$^{-/-}$ ES cells (38) to delineate the dynamics of the increase in *Stra6* transcripts associated with RA treatment of murine ES cells in culture. We demonstrated that there is a 24-fold increase in *Stra6* transcripts 48 h after RA addition in WT ES cells and that this increase does not occur in the *RARγ*$^{-/-}$ ES cells (Fig. 1*A*). We next determined the epigenetic changes that occur along the entire *Stra6* genomic region in response to RA treatment of ES cells. Transcriptional activation is strongly associated with Lys-9/14 acetylation (H3K9/14ac) and Lys-4 trimethylation (H3K4me3) of histone 3 (43). We therefore assessed the dynamics of these epigenetic marks in RA-treated WT and *RARγ*$^{-/-}$ ES cells using ChIP-chip analysis (Fig. 1*B*). At the RefSeq promoter, which we named Promoter$_{\mathrm{Long}}$ (P_L), the increase in H3K9/14ac was much greater in WT than in *RARγ*$^{-/-}$ cells (Fig. 1*B*). At a region ~12 kb downstream of the P_L (RefSeq) promoter, we again observed an RA-dependent increase in the H3K9/14ac epigenetic marks in WT but not in *RARγ*$^{-/-}$ ES cells (Fig. 1*B*). Because this may reflect a downstream promoter driving expression of a shorter transcript, we named this region Promoter$_{\mathrm{Short}}$ (P_S). The H3K4me3 mark was present in both WT and *RARγ*$^{-/-}$ cells at P_L but not at P_S (Fig. 1*B*). We detected increased *Stra6* transcript levels after RA addition only in the WT cells. Thus, the presence of the H3K9/14ac mark correlated with transcriptional activation, whereas the increase in the H3K4me3 mark specifically at P_L was insufficient to induce transcription because the increase in the H3K4me3 mark occurred even in the *RARγ*$^{-/-}$ cells (Fig. 1*B*). In contrast, H3K27me3, a repressive histone modification introduced by the Polycomb repressive complex 2 (PRC2), was decreased at both *Stra6* promoters P_L and P_S in response to RA treatment in the WT but not in the *RARγ*$^{-/-}$ ES cells (Fig. 1*B*). The dynamic changes in these three key histone epigenetic marks revealed two distinct, genomic regions of the *Stra6* gene, which in WT ES cells are remodeled in response to RA.

The Stra6 Gene Encodes Two Transcripts Expressed from Two Distinct Promoters—The data from our ChIP-chip experiments (Fig. 1*B*) pointed to a second regulatory region in the *Stra6* intragenic region, termed P_S. A short form of *Stra6*, which encodes an amino-terminally truncated Stra6 protein, has been identified in human samples (GenBank™ AK092227.1). We hypothesized that the P_S epigenetic "hotspot" located 12 kb downstream of the P_L (RefSeq) reflects transcriptional initiation of a short *Stra6* isoform (*Stra6*$_S$) expressed in mouse ES cells in response to RA.

We designed primers specific for the long and the putative short isoform, respectively, and evaluated the transcript levels of these two *Stra6* isoforms in WT and *RARγ*$^{-/-}$ ES cells in response to RA treatment. The transcript levels of both isoforms were dramatically increased by RA treatment of WT cells, whereas no transcripts were detected in the *RARγ*$^{-/-}$ ES cells (Fig. 1*C*). As a positive control for the induction of *Stra6* by RA, we employed pan-primers to evaluate the total *Stra6* transcript levels (all isoforms) (Fig. 1*C*). To confirm the genotype of the *RARγ* knock-out ES cells, we evaluated the *RARγ* transcript levels in the WT and the *RARγ*$^{-/-}$ ES cells (Fig. 1*C*). The *36B4* transcript levels were used as a reference gene (Fig. 1*C*).

We next determined that the *Stra6* short isoform was generated by a downstream promoter. We used 5′-RACE to identify transcriptional start sites (TSSs) of *Stra6* transcription in WT ES cells before and after treatment with RA. We identified two TSSs ~560 and ~300 bp upstream of the Stra6(−)B primer binding site (Fig. 1*C*, *right*). The 5′-RACE PCR products are slightly larger than the expected sizes of the long and the short isoform of *Stra6* (521 and 261 bp) due to the addition of a 5′-linker (41 bp). Thus, our data show that the two TSSs give rise to the long and a short isoforms of *Stra6*, both of which increased in WT but not in *RARγ*$^{-/-}$ ES cells after RA addition (Fig. 1*C*). We conclude that in WT ES cells, a long and a short *Stra6* transcript are generated from two different promoters, the P_L and the P_S promoter, respectively (shown in Fig. 1*B*, *red bars* at the *bottom*). The levels of both transcripts increase upon RA treatment of WT ES cells (Fig. 1*C*). The *Stra6* transcripts originating from the P_L and the P_S promoters are designated *Stra6*$_L$ (*Stra6.1*) and *Stra6*$_S$ (*Stra6.5*), respectively (Fig. 1*D*). Transcript levels of *Stra6.2*, *Stra6.3*, and *Stra6.4* were below detection in ES cells (data not shown).

Transcriptional Activation Assays Reveal an RARE Proximal to the Promoter of the Stra6$_S$ *Isoform*—We next cloned putative promoter regions of *Stra6* upstream of the luciferase reporter gene in order to identify the genomic sequences involved in the induction of *Stra6* by RA (Fig. 1*D*). We performed transient transfection assays in WT ES cells and evaluated conserved regions proximal to P_L (0.6 kb) and P_S (1.7 and 1.0 kb) for RA-responsive transcriptional activity (1 μM RA, 24 h). In order to evaluate potential enhancer activity of P_S, we included a construct in which P_S is located downstream of the P_L TSS, thereby modeling transcription of the long *Stra6* isoform. We found that P_S was induced to a greater extent than P_L by RA (~5-fold *versus* 2-fold, respectively), whereas P_S failed to enhance the promoter activity of P_L (1.3-fold) (Fig. 1*D*). These transient transfection assays confirmed the presence of an unannotated RA-inducible promoter (P_S), which is located ~12 kb downstream of the RefSeq promoter (P_L) identified in the NCBI database (Fig. 1, *B* and *D*).

We next cloned various regions proximal to the *Stra6* P_S upstream of the reporter luciferase gene and performed transient transfection assays in WT and *RARγ*$^{-/-}$ ES cells. The cells were cultured in either the absence or presence of RA for 8 or 24 h (Fig. 2). We utilized a variety of deletion constructs in the 1.7-kb region proximal to P_S to demonstrate that the greatest increase in transcriptional activation after RA treatment of WT ES cells occurred when a small, 286-bp region was included (*e.g.* Stra6-0.9, Stra6-0.8, *bracketed* in Fig. 2*C*). The majority of the RA inducibility was lost when we deleted this region (Stra6-0.6, Stra6-0.5) (Fig. 2*B*). In the *RARγ*$^{-/-}$ ES cells, the Stra6-0.8 construct did not result in RA induction of the luciferase reporter (Fig. 2*B*), indicating that this RA-responsive region requires RARγ for transcriptional activity.

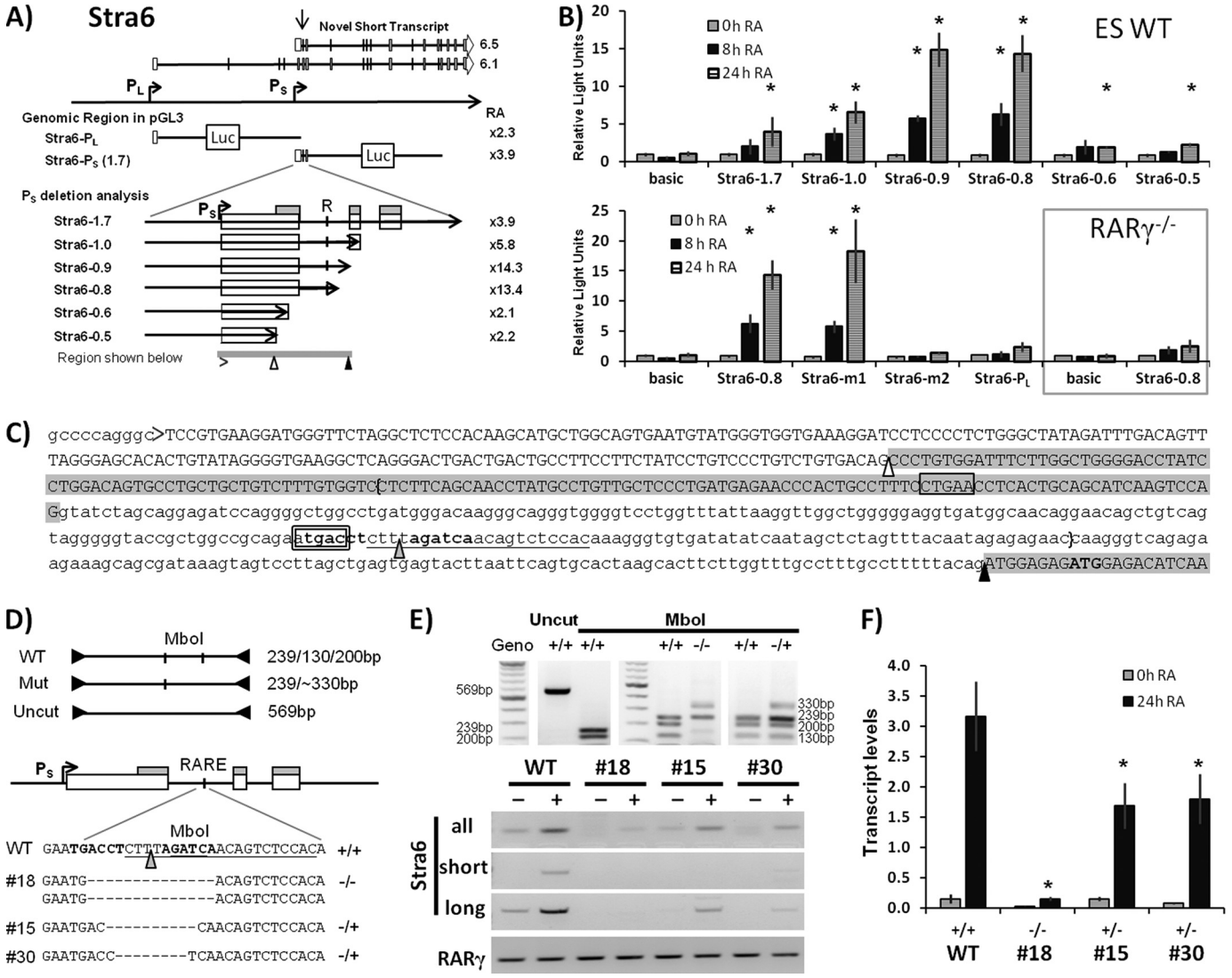

FIGURE 2. **Mapping the RARE of *Stra6* using reporter assays.** *A*, schematic representation of the *Stra6* genomic region and reporter constructs. Promoters for the long and the novel short forms of *Stra6* transcripts are designated as P_L and P_S, respectively. The *arrow* indicates the epigenetic "hotspot" observed in the heat map (Fig. 1). *R*, conserved RARE half-site. A *gray bar below* the schematic reporter construct marks the RA-responsive region shown in *C*. *B*, *Stra6* reporter assays in WT and *RARγ*$^{-/-}$ ES cells upon RA treatment. Deletion analysis of the RA-responsive Stra6-1.7 construct is shown at the *top*. Point-mutated Stra6-0.8 constructs (m1 and m2), the P_L construct, and Stra6-0.8 construct in *RARγ*$^{-/-}$ ES cells (*boxed*) are shown at the *bottom*. Stra6-m1 and Stra6-m2 indicate mutations in RARE half-sites (see details below). All luciferase assays were performed at least three times, starting with fresh cells. *, $p < 0.05$ relative to vehicle control. *C*, key elements of the *Stra6* short isoform proximal to the essential region identified through the reporter assays (*bracketed*): the transcriptional start site (*i.e.* the 5′-end of the transcript) (>), the conserved RARE half-site with the inverted repeat shown in *boldface type* (*double boxed*, m2, TGA → ACT), the non-essential RARE half-site (*boxed*, m1, TGA → ACT), and the putative start codon (*boldface type*). Exon sequences are depicted in *capital letters* with *gray shades* indicating exonic regions present in both $Stra6_S$ and $Stra6_L$. The △, splice acceptor site for splicing of the longer isoforms (in which case the upstream region of this exon is spliced out). ▲, splice acceptor site common for the short (6.5) and the longer (6.1) *Stra6* isoforms. *D*, diagram of the screening strategy and sequences of CRISPR modified ES clones. The CRISPR targeting sequence is *underlined*, and the site of double-stranded breakage is indicated by a *gray triangle*. The genomic sequences of three clones are depicted (one biallelic and two monoallelic mutations). Note that only the mutated allele is shown. *E*, PCR screening and expression of *Stra6* isoforms in ES cell lines with mutated RAREs. *F*, transcriptional induction of *Stra6* in ES cell lines with mutated RAREs. The induction of *Stra6* by RA was impaired in cell lines with monoallelic mutations and strongly impaired in the cell line with biallelic mutations in the *Stra6* RARE (*, $p < 0.05$ relative to RA-treated WT cells). *Stra6* transcript levels were normalized to the *36B4* reference gene. *Error bars*, S.E.

We analyzed the DNA sequence of the RA-responsive region (Fig. 2*C*, *bracketed*) and identified a conserved RARE half-site, A**TGACC** (boldface type indicating conserved nucleotides), located in this intronic region (Fig. 2*C*, *double-boxed sequence*). When the RARE half-site was mutated, the RA-responsiveness of the Stra6-0.8 reporter construct was abrogated (Fig. 2*B*). The Stra6-m2 contains a triple mutation in which the ATGAC (*double-boxed* in Fig. 2*C*) is mutated to AACTC. We also tested another RARE half-site (CTGAA; *boxed* in Fig. 2*C*). Again, we introduced a triple mutation (CTGAA to CACTA), but this mutation did not affect the RA-responsiveness of the Stra6 – 0.8 reporter construct (Fig. 2*B*). Thus, the ATGAC half-site is responsible for the RA-responsiveness of the P_S *Stra6* promoter (Fig. 2*A*).

In summary, we found that a 0.8-kb region proximal to P_S was sufficient to drive a large increase (~13-fold) in luciferase reporter gene expression in response to RA (Fig. 2) and that this increase required RARγ. We further identified an RARE half-site, which, when mutated, abolished the RA-responsiveness of the reporter construct.

TABLE 3

Transcription factors and epigenetic marks associated with *Stra6* promoters in ES cells

The table summarizes the effects of RA on the epigenetic signatures of $Stra6_L$ and $Stra6_S$ promoters in WT and $RAR\gamma^{-/-}$ ES cells (the data are presented in Figs. 1*B* and 4).

Epigenetic mark	Stra6 P_L	Stra6 P_S	Approach
H3K4me3	RA-dependent increase in WT and $RAR\gamma^{-/-}$	No detectable changes	ChIP-chip
H3K9/K14ac	RA-dependent increase in WT and to a lesser extent in $RAR\gamma^{-/-}$	RA-dependent increase in WT and to a lesser extent in $RAR\gamma^{-/-}$	ChIP-chip
p300	RA dependent increase in WT but not in $RAR\gamma^{-/-}$	RA-dependent increase in WT but not in $RAR\gamma^{-/-}$	ChIP-qPCR
H3K27ac	RA-dependent increase in WT and to a lesser extent in $RAR\gamma^{-/-}$	RA-dependent increase in WT and to a lesser extent in $RAR\gamma^{-/-}$	ChIP-qPCR
H3K27me3	RA-dependent depletion in WT but less in $RAR\gamma^{-/-}$	RA-dependent depletion in WT but not in $RAR\gamma^{-/-}$	ChIP-chip, ChIP-qPCR
Suz12	RA-dependent depletion in WT but not in $RAR\gamma^{-/-}$	RA-dependent depletion in WT but less in $RAR\gamma^{-/-}$	ChIP-qPCR
RARγ	No detectable changes	RA-dependent increase in WT	ChIP-qPCR
RXRα	No detectable changes	RA-dependent increase in WT and to a lesser extent in $RAR\gamma^{-/-}$	ChIP-qPCR
PolII-CTD	RA-dependent increase in WT but not in $RAR\gamma^{-/-}$	RA-dependent increase in WT but not in $RAR\gamma^{-/-}$	ChIP-qPCR

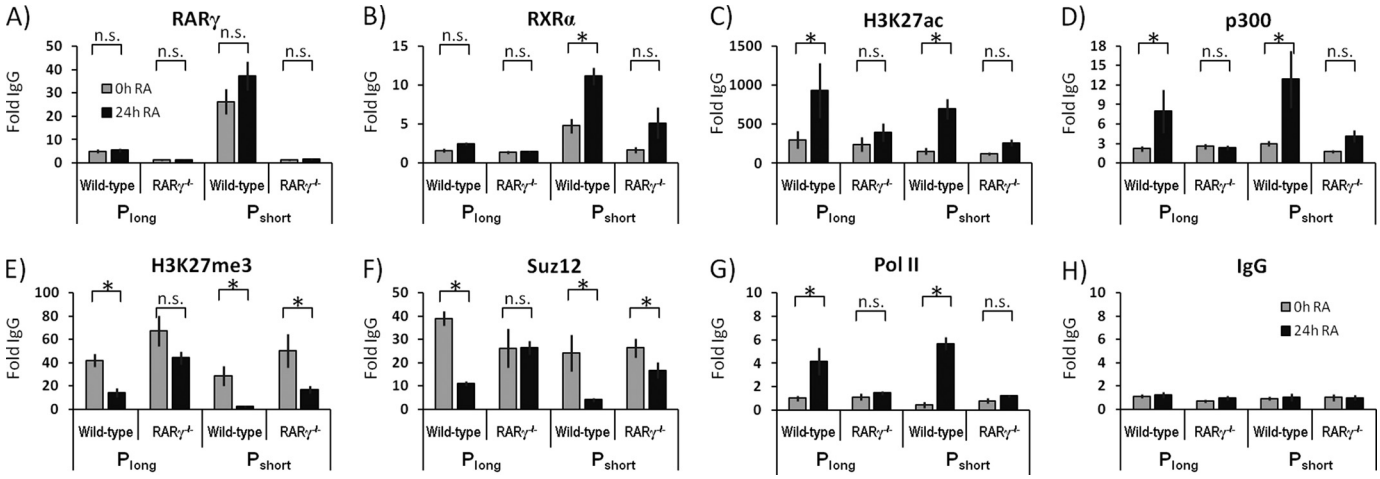

FIGURE 3. **Epigenetic signatures of the *Stra6* gene in WT and $RAR\gamma^{-/-}$ ES cells upon RA treatment.** Chromatin association with *Stra6* P_L and *Stra6* P_S regions in WT and $RAR\gamma^{-/-}$ ES cells treated with vehicle control or RA. *A*, RARγ; *B*, RXRα; *C*, H3K27ac; *D*, p300; *E*, H3K27me3; *F*, Suz12; *G*, RNA polymerase II; *H*, IgG (negative control). All ChIP experiments were performed at least three times, starting with fresh cells ($n \geq 3$). *Gray bars*, untreated cells; *black bars*, cells after 24 h of RA treatment. The IgG ChIP is a negative control. See Fig. 1 for the genomic locations of the ChIP regions. Note the variable *x* axes in different *panels*. *, $p < 0.05$; *n.s.*, not statistically significant. *Error bars*, S.E.

The Stra6 RARE Is Required for Induction of Endogenous Stra6 by RA in ES Cells—We next wanted to address the role of the endogenous RARE in RA-induced transcription of *Stra6*. We employed the CRISPR-Cas9 technology to introduce a targeted deletion of the *Stra6* RARE (Fig. 2*D*) in WT ES cells. We evaluated independent clones for RA-responsive transcription of *Stra6* and found that ablating the *Stra6* RARE resulted in impaired induction of both $Stra6_S$ and $Stra6_L$ (Fig. 2*E*). The cell lines harboring monoallelic or biallelic deletion of the *Stra6* RARE exhibited ~45 and 95% reduction, respectively, in the total *Stra6* transcript levels (all isoforms) relative to RA-stimulated WT ES cells (Fig. 2*F*).

The Stra6 Promoters, P_S and P_L, Show Differential Epigenetic Responses to RA in WT Versus $RAR\gamma^{-/-}$ ES Cells—The consensus RARE element is composed of two direct repeats (RGKTSAN$_{2/5}$RGKTSA). In contrast, the RARE half-site identified in the reporter assays is part of an inverted repeat, (gaaTGACCTctttAGATCAaca, half-sites in capital letters; see the legend to Fig. 2 for details). We therefore evaluated the RARγ and RXRα association with the *Stra6* P_S and P_L regions by ChIP. We show that RARγ and RXRα associate with the P_S promoter region in the WT cells but not in the $RAR\gamma^{-/-}$ ES cells (Fig. 3, *A* and *B*). H3K27ac, generally a mark of enhancers/transcriptional activation (44, 45), occurred at higher levels at both the P_S and P_L regions following RA addition to the WT cells but not the $RAR\gamma^{-/-}$ cells (Fig. 3*C*). The acetylation of H3K27 correlated with coactivator protein p300 association (Fig. 3*D*), which indicates a role for p300 in introducing this histone modification (46).

We detected the H3K27me3 epigenetic mark in both WT and $RAR\gamma^{-/-}$ ES cells; this mark showed a dramatic decrease upon RA addition at both the *Stra6* P_S and P_L regions in WT, whereas higher levels were observed in the $RAR\gamma^{-/-}$ cells relative to WT (Fig. 3*E*). The trimethylation of H3K27 correlated with the levels of the Polycomb group protein Suz12 (Fig. 3*D*), a key component of the Polycomb repressive complex 2 that trimethylates H3K27 (47).

Finally, we evaluated the levels of PolII at the *Stra6* P_S and P_L regions. We demonstrate that at both the *Stra6* P_S and P_L regions, the PolII association increased greatly in WT cells upon RA addition (Fig. 3*G*). This increase was not seen in the $RAR\gamma^{-/-}$ ES cells (Fig. 3*G*). The IgG ChIP, a negative control, demonstrates that the background levels of nonspecific ChIP signals do not change in response to RA (Fig. 3*H*).

Thus, from our ChIP-chip and ChIP-qPCR assays, we conclude that among the evaluated histone marks, the greatest difference between *Stra6* promoters P_L and P_S relates to the H3K4me3 mark. Specifically, the H3K4me3 levels increased at P_L in an RA-dependent manner in both WT and $RAR\gamma^{-/-}$ ES

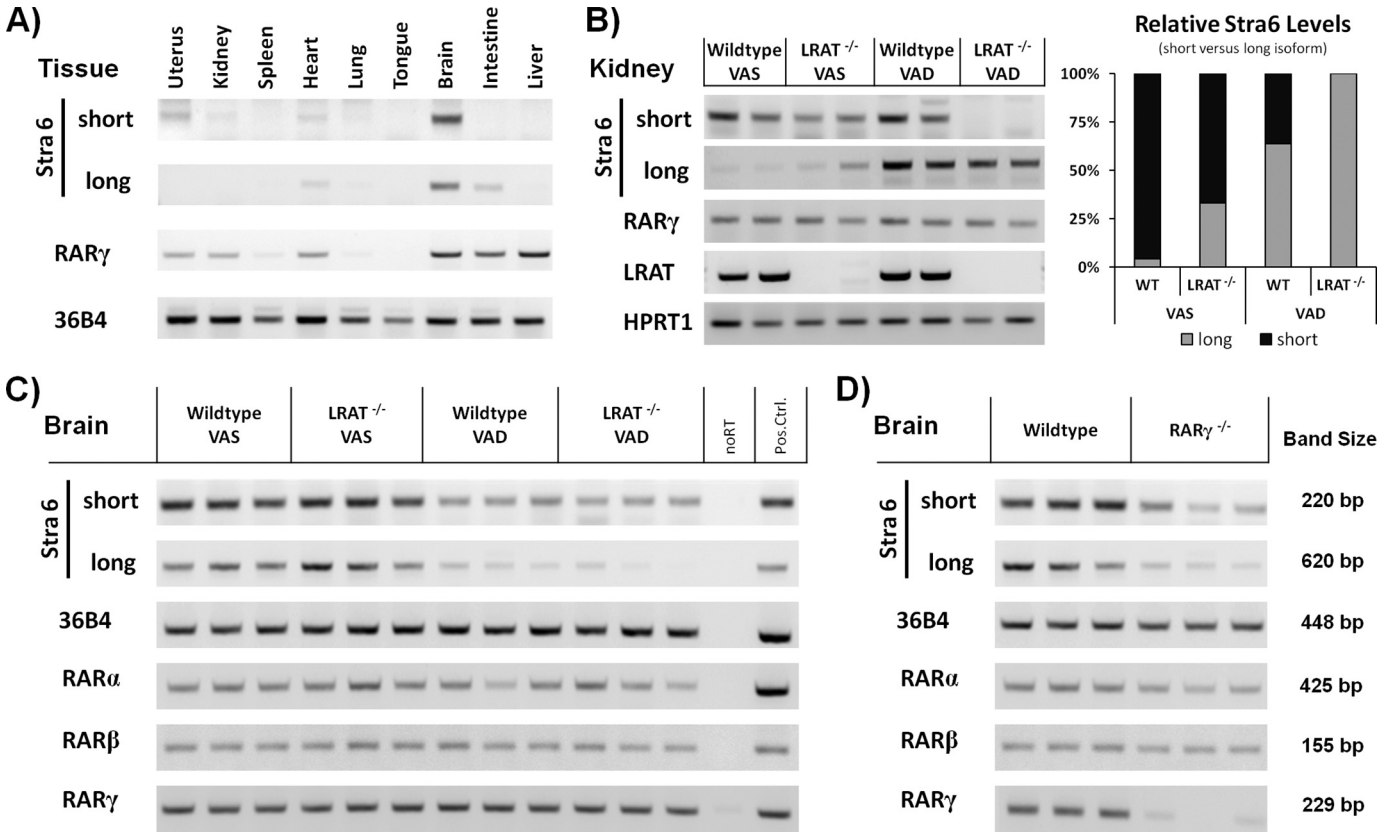

FIGURE 4. **Tissue-specific expression of *Stra6* alternative splice isoforms.** *A*, tissue-specific expression of $Stra6_L$ and $Stra6_S$ in WT mouse tissues. The brain exhibits the highest levels of both transcripts of all of the tissues we examined. *RARγ* transcripts are detected in several tissues, yet *Stra6* is detected only in a subset of these. Transcript levels of the *36B4* reference gene are shown at the *bottom*. Representative data are presented. *B*, vitamin A deficiency is associated with a shift in *Stra6* promoter usage. Transcript levels of the $Stra6_L$ isoform are increased in the kidneys of vitamin A-deficient mice. Transcript levels of the $Stra6_S$ isoform are decreased in the LRAT null animals on normal diet and below detection in vitamin A-deficient LRAT null animals. No change in *RARγ* transcript levels was observed in response to vitamin A deficiency. Transcript levels of *LRAT* (genotyping control on liver samples) and *HPRT1* (loading control) are shown at the *bottom*. Representative data from eight animals are shown. The relative levels of the $Stra6_S$ and $Stra6_L$ isoforms are plotted to the *right*. *C*, transcript levels of both the $Stra6_L$ and $Stra6_S$ isoforms are decreased in the brains of vitamin A-deficient mice. The transcript levels of *RARγ* (and *RARβ*) did not change, whereas RARα transcript levels decreased slightly in response to vitamin A deficiency. Transcript levels of the 36B4 reference gene are included. Data from 12 animals are shown. *D*, $Stra6_L$ and $Stra6_S$ transcript levels are decreased in the brains of *RARγ* null mice. The knockout of *RARγ* was associated also with minor decreases in *RARβ* and *RARα* transcript levels in the brain. Transcript levels of the *36B4* reference gene are included. Data from six animals are shown. *Error bars*, S.E.

cells, whereas at P_S, the H3K4me3 levels did not change in response to RA (Fig. 1*B*). Importantly, whereas we detected no RARγ and RXRα association with P_L, both receptors showed strong association with the P_S proximal promoter region (Fig. 3, *A* and *B*). The epigenetic signatures of *Stra6* P_S and P_L are summarized in Table 3.

The Stra6 Short Isoform mRNA Is Highly Expressed in Brain and Is Reduced in Vitamin A Deficiency—We next asked if the short *Stra6* isoform is expressed in animals and, if so, in what tissues. We determined the levels of $Stra6_S$ and $Stra6_L$ transcripts by RT-PCR in various tissues of WT mice (Fig. 4*A*). We detected $Stra6_L$ transcripts in the heart, intestine, and brain (Fig. 4*A*). Importantly, we also observed high levels of the $Stra6_S$ transcripts in the brain, uterus, kidney, and heart (Fig. 4*A*). We assessed the *RARγ* transcript levels in these tissues (Fig. 4*A*) and found that the $Stra6_S$ and $Stra6_L$ transcripts are present in a subset of the tissues that are positive for *RARγ* transcripts. This supports a role for *RARγ* in regulating the transcription of both *Stra6* isoforms.

Vitamin A-deficient Mice Display Aberrant Stra6 Transcript Levels in Brain and Kidneys—We investigated whether the $Stra6_S$ and $Stra6_L$ transcript levels were differentially regulated in response to vitamin A deficiency. We tested the effects of vitamin A deficiency on *Stra6* transcript levels by placing WT and $LRAT^{-/-}$ C57Bl/6 male and female mice on a vitamin A-deficient diet for 10 weeks and compared these mice with controls fed a normal (vitamin A-sufficient) chow diet. We previously showed that $LRAT^{-/-}$ mice become VAD more rapidly because they are unable to store retinol in the ester form in the liver and other tissues that act as storage depots for retinyl esters (6). We found greatly increased $Stra6_L$ transcript levels in kidneys of WT and $LRAT^{-/-}$ mice that were deprived of vitamin A (Fig. 4*B*) and decreased levels of $Stra6_S$ transcripts in the kidneys of $LRAT^{-/-}$ mice relative to the WT mice. This difference was enhanced by vitamin A deficiency, which almost abolished the $Stra6_S$ transcript levels in $LRAT^{-/-}$ mice (Fig. 4*B*). The *RARγ* transcript levels in the kidneys did not change in response to vitamin A deficiency (Fig. 4*B*), suggesting that the changes in *Stra6* transcript levels are not caused by altered levels of *RARγ*. In vitamin A-sufficient conditions (WT-VAS) the $Stra6_S$ is the isoform predominantly expressed in the kidney, but with increasing severity of vitamin A depletion (either genetic, dietary, or combined), we observed a shift from $Stra6_S$ to $Stra6_L$ expression (Fig. 4*B*). We conclude that the *Stra6* gene

exhibits isoform-specific expression (*e.g.* differential promoter usage) in response to the levels of retinol and/or retinol metabolites in the kidney.

In the brains of vitamin A-deficient animals, the levels of both long and short *Stra6* isoforms are decreased (Fig. 4*C*), whereas the *RARβ* and *RARγ* transcript levels did not change in response to vitamin A deficiency in WT and $LRAT^{-/-}$ mice (Fig. 4*C*). Also, we detected decreased levels of both the long and short *Stra6* isoforms in the brains of *RARγ* null mice on a chow diet that contained vitamin A (Fig. 4*D*). Thus, RARγ is necessary for maintaining the normal levels of both $Stra6_S$ and $Stra6_L$ transcripts in the brain.

DISCUSSION

Stra6 is involved in numerous cell signaling pathways and mediates the uptake of retinol from holo-RBP (2). Thus, there is increasing interest in the regulation of *Stra6* expression, the focus of this research. Murine *Stra6* was originally cloned by Bouillet *et al.* (12), who determined that a genomic region 4.5 kb upstream of the RefSeq promoter does not recapitulate the RA inducible transcription of *Stra6*. We have mapped a *Stra6* RARE to a region 12 kb downstream of the RefSeq promoter, and we demonstrate here that two different transcripts are generated from the *Stra6* gene in cultured ES cells and in various murine tissues. In WT ES cells, RA induces transcription of both $Stra6_S$ and $Stra6_L$ through a single RARE (Figs. 1 and 2). Similarly, in the brain, $Stra6_L$ and $Stra6_S$ levels both decrease in response to vitamin A deprivation, but intriguingly, in the kidney, the $Stra6_S$ and $Stra6_L$ transcripts are regulated in an opposing fashion (Fig. 4).

Consistent with the increase in $Stra6_L$ and $Stra6_S$ transcript levels in RA-treated WT ES cells (Fig. 1), we observed RA-dependent increases in PolII levels at both $Stra6_L$ and $Stra6_S$ promoters (Fig. 3). In contrast, RARγ and RXRα showed strong association only with the $Stra6_S$ promoter (Fig. 3*B*). The absence of RAREs proximal to *Stra6*-P_L is supported by our analysis of published ChIP-seq data (48) and is consistent with previous findings (12). We employed CRISPR-Cas9 technology to demonstrate that in ES cells, the *Stra6* RARE, which is located proximal to the $Stra6_S$ promoter, is required for RA-responsive transcription of both $Stra6_S$ and $Stra6_L$ (Fig. 2*E*).

We focused on the epigenetic changes associated with the transcriptional activation of the *Stra6* gene by RA. We found that both $Stra6_L$ and $Stra6_S$ promoters are transcriptionally activated by RA, as evident by an RA-dependent increase in histone acetylation (H3K9/14ac, H3K27ac, and p300) and Polycomb depletion (H3K27me3 and Suz12). Importantly, these marks exhibited no changes when $RAR\gamma^{-/-}$ ES cells were treated with RA (Fig. 3), demonstrating the requirement for RARγ in RA-dependent Polycomb removal and histone acetylation of the *Stra6* genomic region and in the transcriptional activation of *Stra6* in ES cells.

In contrast to histone acetylation, which increased at both *Stra6* P_L and P_S, we observed an RA-associated increase in H3K4me3 levels at the $Stra6_L$ promoter only; notably, the H3K4me3 levels increased even in $RAR\gamma^{-/-}$ ES cells (Fig. 1*B*). The RA-associated increase in H3K4me3 at the $Stra6_L$ promoter is consequently independent of RARγ, and this modification alone is insufficient to induce transcriptional activation of *Stra6*. *LRAT* and *Meis1* display similar transcriptional regulation; RARγ is required for the RA-dependent increase in H3K9/14ac marks, whereas the RA-induced increase in H3K4me3 takes place even in $RAR\gamma^{-/-}$ ES cells (38). In contrast, the Cyp26a1 promoter exhibited lower levels of both H3K4me3 and H3K9/14ac marks in RA-treated $RAR\gamma^{-/-}$ relative to WT ES cells (38). The H3K4me3 modification is deposited by mammalian homologs of the *Drosophila* Trithorax, termed myeloid/lymphoid or mixed-lineage leukemia (MLL) proteins, and in particular, the MLL2 complex plays an important role in differentiation of ES cells (49).

Our data from WT mice on VAS *versus* VAD diets show differences in the regulation of $Stra6_L$ and $Stra6_S$ transcripts in the kidneys (Fig. 4*B*). When retinol is supplied daily in the diet (Fig. 4*B*, VAS), only the $Stra6_S$ transcript is expressed. However, when retinol is not present in the diet for 10 weeks, the $LRAT^{-/-}$ mice become vitamin A-deficient (6), and only the $Stra6_L$ transcript is expressed in the kidneys (Fig. 4*B*, *VAD*, $LRAT^{-/-}$). In WT mice that are on a VAD diet for 10 weeks and are only partially vitamin A-deficient (6), both the $Stra6_L$ and $Stra6_S$ transcripts are expressed (Fig. 4*B*, *Wildtype*, *VAD*). These data show that $Stra6_S$ mRNA is expressed in kidneys when retinol is present in the body but that as retinol stores are depleted in the livers of WT mice during the 10 weeks on the vitamin A-deficient diet, expression of the $Stra6_L$ transcript is activated in the kidneys although retinol is still present in the WT mice. Our data strongly suggest that when circulating retinol is abundant (from dietary uptake), $Stra6_S$ is the predominant isoform expressed in the murine kidneys. In contrast, as retinol stores are depleted as a result of dietary vitamin A deficiency, expression of the $Stra6_L$ isoform increases in the kidneys. The differential regulation of the two *Stra6* transcript isoforms in the kidney in response to vitamin A deprivation points to physiologically distinct functions of the different isoforms in the regulation of retinoid homeostasis.

In the brain, unlike the kidney, both the $Stra6_L$ and $Stra6_S$ transcripts are reduced in both WT and $LRAT^{-/-}$ mice on a vitamin A-deficient diet (Fig. 4*C*). Thus, in the brain, we do not observe the major switch from the $Stra6_S$ to $Stra6_L$ transcripts during vitamin A deficiency that we detected in the kidneys (Fig. 4, *B versus C*). Furthermore, we also show that both the $Stra6_L$ and $Stra6_S$ transcript levels are reduced in the brains of $RAR\gamma^{-/-}$ mice compared with the WT mice (Fig. 4*D*). This is in marked contrast to the elevated levels of *Stra6* observed in RA-treated F9 RARα null cells (35) and in the testicular tubules of *RARα* null mice (12). Consequently, whereas RARγ plays a direct role in activating *Stra6* expression, RARα may function to repress transcription of *Stra6*. Whether loss of RARα results in elevated levels of one or multiple *Stra6* isoforms is not known. The presence of *RARγ* transcripts in each of the tissues where either $Stra6_S$ or $Stra6_L$ transcripts are present (uterus, kidney, heart, brain, and intestine) further supports the dependence of *Stra6* expression on RARγ.

Stra6 expression is directly regulated by RA (Fig. 3*A*) and responds to vitamin A availability *in vivo* (Fig. 4). However, because we observed elevated levels of $Stra6_L$ in the kidneys of vitamin A-deficient animals, we conclude that $Stra6_L$ can be

expressed in a manner independent of RA. This may reflect an additional layer of regulation whereby the kidneys are able to increase $Stra6_L$ levels when faced with vitamin A scarcity.

Our studies identify a shorter *Stra6.5* isoform (Fig. 1), which encodes a putative amino-terminally truncated Stra6 protein (532 amino acids). In contrast, *Stra6.1, Stra6.2*, *Stra6.3*, and *Stra6.4* isoforms all encode identical, larger Stra6 proteins (670 amino acids, NP_001155947.1). The putative $Stra6_S$ protein may share functional properties with the B-chain of human RBPR2, whose protein coding sequence is split onto two separate genes, one encoding the amino-terminal A-chain and one the carboxyl-terminal B-chain, respectively (4). It is interesting to note that RBP4 interactions and retinol uptake are impaired by insertions at residues 16, 84, and 133 in the amino-terminal region of the larger Stra6 protein (50), a region that is absent from $Stra6_S$ (and from the B-chain of RBP2). In contrast, mutations at residues 323, 357, and 548, shared by both *Stra6* isoforms, completely abolished the function of the larger Stra6 protein (50). It is tempting to speculate that the carboxyl-terminal region of Stra6 has a structural role in RBP4 interaction, whereas the amino-terminal region of Stra6 may serve a regulatory function, possibly by distinguishing between apo- and holo-RBP4 (unliganded and liganded, respectively). Importantly, that distinction could be involved in regulating the direction of retinol transport (22). This model suggests that decreasing $Stra6_S$ levels in the kidneys may be a physiological response to vitamin A deprivation to reduce the loss of vitamin A to the urine. Further studies will be needed to characterize the functional differences between the Stra6 proteins encoded by the $Stra6_L$ and $Stra6_S$ transcripts, but our data indicate that the kidneys respond to vitamin A deficiency by differential *Stra6* promoter usage, which may play a major role in the retention of retinol when vitamin A is scarce.

Acknowledgments—We thank Carlos Rodriguez for kidney cDNA, Steven Trasino for assistance in harvesting of mouse tissues and critically reading the manuscript, Tamara Weissman and Dan Stummer for editorial assistance, Dr. Pierre Chambon for the RARγ knock-out mice, and the Gudas laboratory for useful discussions.

REFERENCES

1. O'Byrne, S. M., and Blaner, W. S. (2013) Retinol and retinyl esters: biochemistry and physiology: Thematic Review Series: fat-soluble vitamins: vitamin A. *J. Lipid Res.* **54,** 1731–1743
2. Kawaguchi, R., Yu, J., Honda, J., Hu, J., Whitelegge, J., Ping, P., Wiita, P., Bok, D., and Sun, H. (2007) A membrane receptor for retinol binding protein mediates cellular uptake of vitamin A. *Science* **315,** 820–825
3. Zhong, M., Kawaguchi, R., Ter-Stepanian, M., Kassai, M., and Sun, H. (2013) Vitamin a transport and the transmembrane pore in the cell-surface receptor for plasma retinol binding protein. *PLoS One* **8,** e73838
4. Alapatt, P., Guo, F., Komanetsky, S. M., Wang, S., Cai, J., Sargsyan, A., Rodríguez Díaz, E., Bacon, B. T., Aryal, P., and Graham, T. E. (2013) Liver retinol transporter and receptor for serum retinol-binding protein (RBP4). *J. Biol. Chem.* **288,** 1250–1265
5. Kim, Y. K., Wassef, L., Hamberger, L., Piantedosi, R., Palczewski, K., Blaner, W. S., and Quadro, L. (2008) Retinyl ester formation by lecithin: retinol acyltransferase is a key regulator of retinoid homeostasis in mouse embryogenesis. *J. Biol. Chem.* **283,** 5611–5621
6. Liu, L., and Gudas, L. J. (2005) Disruption of the lecithin:retinol acyltransferase gene makes mice more susceptible to vitamin A deficiency. *J. Biol. Chem.* **280,** 40226–40234
7. Ghyselinck, N. B., Båvik, C., Sapin, V., Mark, M., Bonnier, D., Hindelang, C., Dierich, A., Nilsson, C. B., Håkansson, H., Sauvant, P., Azaïs-Braesco, V., Frasson, M., Picaud, S., and Chambon, P. (1999) Cellular retinol-binding protein I is essential for vitamin A homeostasis. *EMBO J.* **18,** 4903–4914
8. Napoli, J. L., Boerman, M. H., Chai, X., Zhai, Y., and Fiorella, P. D. (1995) Enzymes and binding proteins affecting retinoic acid concentrations. *J. Steroid Biochem. Mol. Biol.* **53,** 497–502
9. O'Byrne, S. M., Wongsiriroj, N., Libien, J., Vogel, S., Goldberg, I. J., Baehr, W., Palczewski, K., and Blaner, W. S. (2005) Retinoid absorption and storage is impaired in mice lacking lecithin:retinol acyltransferase (LRAT). *J. Biol. Chem.* **280,** 35647–35657
10. Amengual, J., Golczak, M., Palczewski, K., and von Lintig, J. (2012) Lecithin:retinol acyl transferase is critical for cellular uptake of vitamin A from serum retinol binding protein. *J. Biol. Chem.* **287,** 24216–24227
11. Wu, L., and Ross, A. C. (2010) Acidic retinoids synergize with vitamin A to enhance retinol uptake and STRA6, LRAT, and CYP26B1 expression in neonatal lung. *J. Lipid Res.* **51,** 378–387
12. Bouillet, P., Sapin, V., Chazaud, C., Messaddeq, N., Décimo, D., Dollé, P., and Chambon, P. (1997) Developmental expression pattern of Stra6, a retinoic acid-responsive gene encoding a new type of membrane protein. *Mech. Dev.* **63,** 173–186
13. Pasutto, F., Sticht, H., Hammersen, G., Gillessen-Kaesbach, G., Fitzpatrick, D. R., Nürnberg, G., Brasch, F., Schirmer-Zimmermann, H., Tolmie, J. L., Chitayat, D., Houge, G., Fernández-Martínez, L., Keating, S., Mortier, G., Hennekam, R. C., von der Wense, A., Slavotinek, A., Meinecke, P., Bitoun, P., Becker, C., Nürnberg, P., Reis, A., and Rauch, A. (2007) Mutations in STRA6 cause a broad spectrum of malformations including anophthalmia, congenital heart defects, diaphragmatic hernia, alveolar capillary dysplasia, lung hypoplasia, and mental retardation. *Am. J. Hum. Genet.* **80,** 550–560
14. Skazik, C., Amann, P. M., Heise, R., Marquardt, Y., Czaja, K., Kim, A., Rühl, R., Kurschat, P., Merk, H. F., Bickers, D. R., and Baron, J. M. (2014) Downregulation of STRA6 expression in epidermal keratinocytes leads to hyperproliferation-associated differentiation in both *in vitro* and *in vivo* skin models. *J. Invest. Dermatol.* **134,** 1579–1588
15. Berry, D. C., Jin, H., Majumdar, A., and Noy, N. (2011) Signaling by vitamin A and retinol-binding protein regulates gene expression to inhibit insulin responses. *Proc. Natl. Acad. Sci. U.S.A.* **108,** 4340–4345
16. Chen, C. H., Hsieh, T. J., Lin, K. D., Lin, H. Y., Lee, M. Y., Hung, W. W., Hsiao, P. J., and Shin, S. J. (2012) Increased unbound retinol-binding protein 4 concentration induces apoptosis through receptor-mediated signaling. *J. Biol. Chem.* **287,** 9694–9707
17. Berry, D. C., O'Byrne, S. M., Vreeland, A. C., Blaner, W. S., and Noy, N. (2012) Cross-talk between signalling and vitamin A transport by the retinol-binding protein receptor STRA6. *Mol. Cell. Biol.* **32,** 3164–3175
18. Carrera, S., Cuadrado-Castano, S., Samuel, J., Jones, G. D., Villar, E., Lee, S. W., and Macip, S. (2013) Stra6, a retinoic acid-responsive gene, participates in p53-induced apoptosis after DNA damage. *Cell Death Differ.* **20,** 910–919
19. Muenzner, M., Tuvia, N., Deutschmann, C., Witte, N., Tolkachov, A., Valai, A., Henze, A., Sander, L. E., Raila, J., and Schupp, M. (2013) Retinol-binding protein 4 and its membrane receptor STRA6 control adipogenesis by regulating cellular retinoid homeostasis and retinoic acid receptor α activity. *Mol. Cell. Biol.* **33,** 4068–4082
20. Golzio, C., Martinovic-Bouriel, J., Thomas, S., Mougou-Zrelli, S., Grattagliano-Bessieres, B., Bonniere, M., Delahaye, S., Munnich, A., Encha-Razavi, F., Lyonnet, S., Vekemans, M., Attie-Bitach, T., and Etchevers, H. C. (2007) Matthew-Wood syndrome is caused by truncating mutations in the retinol-binding protein receptor gene STRA6. *Am. J. Hum. Genet.* **80,** 1179–1187
21. Chassaing, N., Golzio, C., Odent, S., Lequeux, L., Vigouroux, A., Martinovic-Bouriel, J., Tiziano, F. D., Masini, L., Piro, F., Maragliano, G., Delezoide, A. L., Attié-Bitach, T., Manouvrier-Hanu, S., Etchevers, H. C., and Calvas, P. (2009) Phenotypic spectrum of STRA6 mutations: from Matthew-Wood syndrome to non-lethal anophthalmia. *Hum. Mutat.* **30,** E673–E681

22. Kawaguchi, R., Zhong, M., Kassai, M., Ter-Stepanian, M., and Sun, H. (2013) Differential and isomer-specific modulation of vitamin A transport and the catalytic activities of the RBP receptor by retinoids. *J. Membr. Biol.* **246,** 647–660
23. Kawaguchi, R., Yu, J., Wiita, P., Honda, J., and Sun, H. (2008) An essential ligand-binding domain in the membrane receptor for retinol-binding protein revealed by large-scale mutagenesis and a human polymorphism. *J. Biol. Chem.* **283,** 15160–15168
24. Chassaing, N., Ragge, N., Kariminejad, A., Buffet, A., Ghaderi-Sohi, S., Martinovic, J., and Calvas, P. (2013) Mutation analysis of the STRA6 gene in isolated and non-isolated anophthalmia/microphthalmia. *Clin. Genet.* **83,** 244–250
25. Ruiz, A., Mark, M., Jacobs, H., Klopfenstein, M., Hu, J., Lloyd, M., Habib, S., Tosha, C., Radu, R. A., Ghyselinck, N. B., Nusinowitz, S., and Bok, D. (2012) Retinoid content, visual responses, and ocular morphology are compromised in the retinas of mice lacking the retinol-binding protein receptor, STRA6. *Invest. Ophthalmol. Vis. Sci.* **53,** 3027–3039
26. Berry, D. C., Jacobs, H., Marwarha, G., Gely-Pernot, A., O'Byrne, S. M., DeSantis, D., Klopfenstein, M., Feret, B., Dennefeld, C., Blaner, W. S., Croniger, C. M., Mark, M., Noy, N., and Ghyselinck, N. B. (2013) The STRA6 receptor is essential for retinol-binding protein-induced insulin resistance but not for maintaining vitamin A homeostasis in tissues other than the eye. *J. Biol. Chem.* **288,** 24528–24539
27. Amengual, J., Zhang, N., Kemerer, M., Maeda, T., Palczewski, K., and Von Lintig, J. (2014) STRA6 is critical for cellular vitamin A uptake and homeostasis. *Hum. Mol. Genet.* **23,** 5402–5417
28. Zemany, L., Kraus, B. J., Norseen, J., Saito, T., Peroni, O. D., Johnson, R. L., and Kahn, B. B. (2014) Downregulation of STRA6 in adipocytes and adipose stromovascular fraction in obesity and effects of adipocyte-specific STRA6 knockdown *in vivo*. *Mol. Cell. Biol.* **34,** 1170–1186
29. Norseen, J., Hosooka, T., Hammarstedt, A., Yore, M. M., Kant, S., Aryal, P., Kiernan, U. A., Phillips, D. A., Maruyama, H., Kraus, B. J., Usheva, A., Davis, R. J., Smith, U., and Kahn, B. B. (2012) Retinol-binding protein 4 inhibits insulin signaling in adipocytes by inducing proinflammatory cytokines in macrophages through a c-Jun N-terminal kinase- and Toll-like receptor 4-dependent and retinol-independent mechanism. *Mol. Cell. Biol.* **32,** 2010–2019
30. Urvalek, A., Laursen, K. B., and Gudas, L. J. (2014) The roles of retinoic acid and retinoic acid receptors in inducing epigenetic changes. *Subcell. Biochem.* **70,** 129–149
31. Gudas, L. J. (2012) Emerging roles for retinoids in regeneration and differentiation in normal and disease states. *Biochim. Biophys. Acta* **1821,** 213–221
32. Mongan, N. P., and Gudas, L. J. (2007) Diverse actions of retinoid receptors in cancer prevention and treatment. *Differentiation* **75,** 853–870
33. Kashyap, V., Gudas, L. J., Brenet, F., Funk, P., Viale, A., and Scandura, J. M. (2011) Epigenomic reorganization of the clustered Hox genes in embryonic stem cells induced by retinoic acid. *J. Biol. Chem.* **286,** 3250–3260
34. Laursen, K. B., Mongan, N. P., Zhuang, Y., Ng, M. M., Benoit, Y. D., and Gudas, L. J. (2013) Polycomb recruitment attenuates retinoic acid-induced transcription of the bivalent NR2F1 gene. *Nucleic Acids Res.* **41,** 6430–6443
35. Taneja, R., Bouillet, P., Boylan, J. F., Gaub, M. P., Roy, B., Gudas, L. J., and Chambon, P. (1995) Reexpression of retinoic acid receptor (RAR) γ or overexpression of RAR α or RAR β in RAR γ-null F9 cells reveals a partial functional redundancy between the three RAR types. *Proc. Natl. Acad. Sci. U.S.A.* **92,** 7854–7858
36. Boylan, J. F., Lohnes, D., Taneja, R., Chambon, P., and Gudas, L. J. (1993) Loss of retinoic acid receptor γ function in F9 cells by gene disruption results in aberrant Hoxa-1 expression and differentiation upon retinoic acid treatment. *Proc. Natl. Acad. Sci. U.S.A.* **90,** 9601–9605
37. Faria, T. N., Mendelsohn, C., Chambon, P., and Gudas, L. J. (1999) The targeted disruption of both alleles of RARβ(2) in F9 cells results in the loss of retinoic acid-associated growth arrest. *J. Biol. Chem.* **274,** 26783–26788
38. Kashyap, V., Laursen, K. B., Brenet, F., Viale, A. J., Scandura, J. M., and Gudas, L. J. (2013) RARγ is essential for retinoic acid induced chromatin remodeling and transcriptional activation in embryonic stem cells. *J. Cell Sci.* **126,** 999–1008
39. Cong, L., Ran, F. A., Cox, D., Lin, S., Barretto, R., Habib, N., Hsu, P. D., Wu, X., Jiang, W., Marraffini, L. A., and Zhang, F. (2013) Multiplex genome engineering using CRISPR/Cas systems. *Science* **339,** 819–823
40. Gillespie, R. F., and Gudas, L. J. (2007) Retinoid regulated association of transcriptional co-regulators and the Polycomb group protein SUZ12 with the retinoic acid response elements of Hoxa1, RARβ(2), and Cyp26A1 in F9 embryonal carcinoma cells. *J. Mol. Biol.* **372,** 298–316
41. Kashyap, V., and Gudas, L. J. (2010) Epigenetic regulatory mechanisms distinguish retinoic acid-mediated transcriptional responses in stem cells and fibroblasts. *J. Biol. Chem.* **285,** 14534–14548
42. Laursen, K. B., Wong, P. M., and Gudas, L. J. (2012) Epigenetic regulation by RARα maintains ligand-independent transcriptional activity. *Nucleic Acids Res.* **40,** 102–115
43. Barski, A., Cuddapah, S., Cui, K., Roh, T. Y., Schones, D. E., Wang, Z., Wei, G., Chepelev, I., and Zhao, K. (2007) High-resolution profiling of histone methylations in the human genome. *Cell* **129,** 823–837
44. Verdone, L., Agricola, E., Caserta, M., and Di Mauro, E. (2006) Histone acetylation in gene regulation. *Brief Funct. Genomic. Proteomic.* **5,** 209–221
45. Guillemette, B., Drogaris, P., Lin, H. H., Armstrong, H., Hiragami-Hamada, K., Imhof, A., Bonneil, E., Thibault, P., Verreault, A., and Festenstein, R. J. (2011) H3 lysine 4 is acetylated at active gene promoters and is regulated by H3 lysine 4 methylation. *PLoS Genet.* **7,** e1001354
46. Holmqvist, P. H., and Mannervik, M. (2013) Genomic occupancy of the transcriptional co-activators p300 and CBP. *Transcription* **4,** 18–23
47. Pasini, D., Bracken, A. P., Jensen, M. R., Lazzerini Denchi, E., and Helin, K. (2004) Suz12 is essential for mouse development and for EZH2 histone methyltransferase activity. *EMBO J.* **23,** 4061–4071
48. Mendoza-Parra, M. A., Walia, M., Sankar, M., and Gronemeyer, H. (2011) Dissecting the retinoid-induced differentiation of F9 embryonal stem cells by integrative genomics. *Mol. Syst. Biol.* **7,** 538
49. Denissov, S., Hofemeister, H., Marks, H., Kranz, A., Ciotta, G., Singh, S., Anastassiadis, K., Stunnenberg, H. G., and Stewart, A. F. (2014) Mll2 is required for H3K4 trimethylation on bivalent promoters in embryonic stem cells, whereas Mll1 is redundant. *Development* **141,** 526–537
50. Kawaguchi, R., Yu, J., Wiita, P., Ter-Stepanian, M., and Sun, H. (2008) Mapping the membrane topology and extracellular ligand binding domains of the retinol binding protein receptor. *Biochemistry* **47,** 5387–5395